Available online at www.sciencedirect.com
ScienceDirect
Journal of Sound and Vibration 319 (2009) 1097–1106
JOURNAL OF SOUND AND VIBRATION
www.elsevier.com/locate/jsvi

End correction at the interface between a plain and a perforated pipe

K.S. Peat*

Department of Aeronautical and Automotive Engineering, Loughborough University, Loughborough, Leicestershire LE11 3TU, UK

Received 10 April 2008; received in revised form 26 June 2008; accepted 30 June 2008
Handling Editor: C.L. Morfey
Available online 13 August 2008

Abstract

This paper considers the plane-wave end correction that should be applied at the junction between a plain and a perforated pipe of equal diameter in the absence of mean flow. A general theory is developed that results in an equation for the end correction of all such junctions. The theory is verified by experimental results for the end correction obtained via the measurement of resonant frequency of a Helmholtz resonator whose neck is formed of a plain section and then a perforated section of pipe, before termination into free space. It is shown that in most practical situations within automotive silencers the perforated pipe will be long enough for the nature of the termination to be irrelevant. A simple formula is developed to evaluate this long-length limit and from it the dependence of the end correction upon all the parameters within the problem becomes explicit.
© 2008 Elsevier Ltd. All rights reserved.

1. Introduction

Any geometrical discontinuity in a duct system, such as a pipe termination or an area expansion, will generate non-planar waves. At low frequencies, below that of the lowest cut-on frequency of a non-planar wave, these non-planar waves will be evanescent such that the acoustic performance of a duct system can be predicted by a simple plane-wave analysis. However, it is possible to improve the accuracy of a plane-wave analysis by the use of discontinuity impedances that account for the generation of evanescent waves at each given geometric discontinuity. In the absence of any mean flow through the duct system, any geometric discontinuity has negligible acoustic resistance. Hence, the discontinuity impedance is essentially a reactance whose effect is equivalent to an assumed small increase in duct length, a so-called 'end correction'. Thus, the effective acoustic length of a duct is the sum of its physical length and any appropriate end corrections at each end of the duct. Knowledge of the end corrections of a duct is therefore of fundamental importance in the determination of its resonant frequencies, which are characterised by the effective acoustic length of the duct. Two classic cases of end corrections are an open duct termination into free space [1] and a flanged duct termination into half-space [2]. Within duct systems, geometric discontinuities often take the form of a change

*Tel.: +44 1509 227232; fax: +44 1509 227275.
E-mail address: K.S.Peat@lboro.ac.uk

0022-460X/$ - see front matter © 2008 Elsevier Ltd. All rights reserved.
doi:10.1016/j.jsv.2008.06.055

of cross-sectional area, see Fig. 1. The full open or flanged duct end correction is then reduced by the Karal correction factor [3], which is a function of the area ratio at the discontinuity. For the system given in Fig. 1, the pipes of physical lengths L_1 and L_2 should each have end corrections added at both ends to give the effective acoustic length for accurate evaluation of the systems of half-wave resonances in the open–open tubes. In addition, the physical length L_3 needs to be increased by a single end correction to give the precise frequencies of the quarter-wave system of resonances of the closed–open tube formed by the extended outlet. Clearly, the greater the ratio of end corrections to physical length for a given duct, the greater will be the error in determination of the resonant frequencies if end corrections are ignored or not known accurately. The lengths of extended inlets and outlets are usually chosen to tune out specific frequencies and often these lengths are quite small, so inclusion of an accurate end correction can be vital.

Within flow ducts, it is unusual to find a simple expansion box silencer of the form given in Fig. 1. The reason for this is that there would be large flow resistance at the inlet as the flow separates and expands into the wider duct, with associated eddies. Flow resistance at the outlet can also be significant. In order to reduce flow resistance, a perforated tube is used to bridge the gap between the flow inlet and outlet, as shown in Fig. 2, such that the mean flow is mostly confined within the central tube. The perforations enable acoustic waves to propagate from inner to outer duct.

Given knowledge of the impedance of the perforate, it is possible to conduct an approximate plane-wave analysis of a silencer such as that given in Fig. 2 by either a segmentation [4] or a decoupling [5] approach. However, if the end correction for a perforate were known, a designer could precisely determine the physical length of extended inlet or outlet required to tune out a particular frequency without recourse to trial and error using a full plane-wave analysis of the system.

A very common type of rear box silencer on road vehicles is some form of triple-pass silencer such as shown in Fig. 3. Here, the flow return volumes at either end of the silencer become Helmholtz resonators with two

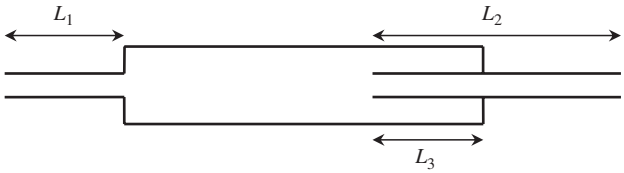

Fig. 1. Simple expansion chamber silencer.

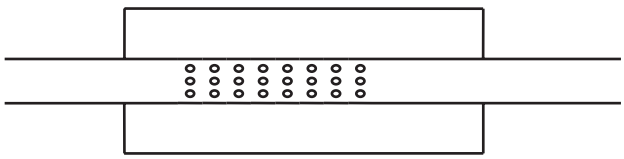

Fig. 2. Typical flow-duct expansion chamber silencer.

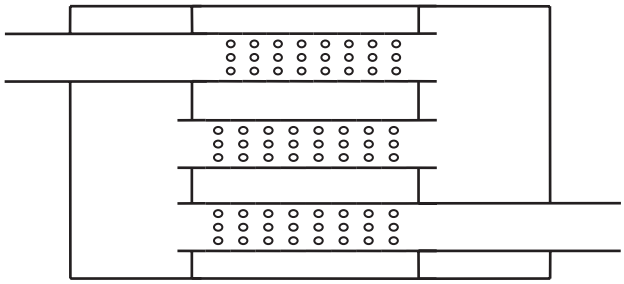

Fig. 3. Typical triple-pass silencer box.

necks, each of which terminate in a perforated tube. Typically, these necks are very short and hence the end corrections of the necks can dominate the effective acoustic length of the necks and thereby the resonant frequency of the Helmholtz chamber. Again, a silencer designer will wish to tune these Helmholtz resonators to specific frequencies and thus knowledge of the end correction where the plain tube of the neck meets the perforated tube is necessary.

There is very little previous work on the topic of end corrections at the junction of plain with perforated tubes. The first [6] was based upon a finite element analysis of a silencer of the form given in Fig. 2. Mean flow effects were included, but the mean flow was assumed to be inviscid and irrotational. Values of end correction as a function of the porosity of the perforate were based upon numerical experiments for one size of silencer only. The results indicated that the perforated tube has a significant effect on the end correction and one that increases as the mean flow increases. The only other known previous work [7] was a purely experimental investigation that utilised a Helmholtz resonator with two necks, one of which terminated in a perforated pipe, such that air could be forced through the system. Thus, experimental results of the end correction due to a variety of perforated pipes were found with and without mean flow effects.

The problem with both numerical and experimental approaches to this problem is that the number of variables in the problem is very large, such that any set of results obtained are specific to a small subset of all possible cases. The approach taken in this paper is to develop a theoretical formula for the end correction which will be generally applicable to any perforate type and pipe size. However, for the moment attention has been restricted to the case of zero mean flow. Experimental results from a selection of perforates have been obtained and it is found that these validate the theory. Finally, theoretical analysis is used to establish some general results about the end corrections due to perforates and simplified formulae for evaluation.

2. Theory

Consider low-frequency plane-wave acoustic propagation in a uniform plain pipe of radius a that connects to a perforated pipe of similar radius at some plane I, see Fig. 4a. The perforated pipe is assumed to consist of n identical sections, where each section has a single ring of N circular holes of radius b followed by a plain pipe section of length L and radius a, see Fig. 4b. For a general section j, the acoustic pressure p and particle

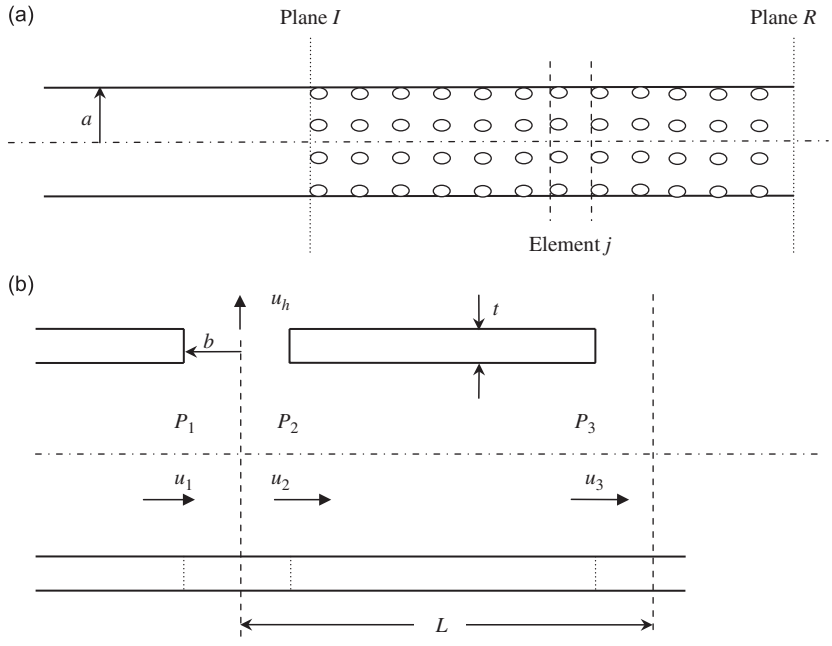

Fig. 4. (a) Pipe termination and perforate. (b) General jth element of the perforate.

velocity u of the plane wave before (subscript 1) and after (subscript 2) the ring of holes are related by

$$p_1 = p_2 \tag{1}$$

and

$$a^2 u_1 = a^2 u_2 + N b^2 u_h, \tag{2}$$

where u_h is the particle velocity through each hole. Eqs. (1) and (2) express continuity of acoustic pressure and volume velocity across the ring of apertures and can be expressed in matrix form as

$$\begin{bmatrix} p_1 \\ \rho c u_1 \end{bmatrix} = \begin{bmatrix} 1 & 0 \\ \dfrac{N}{\zeta_h}\left(\dfrac{b}{a}\right)^2 & 1 \end{bmatrix} \begin{bmatrix} p_2 \\ \rho c u_2 \end{bmatrix}, \tag{3}$$

where $\zeta_h = p_1/\rho c u_h$ is the specific impedance of a single hole, c the speed of sound and ρ the mean density. Similarly, the acoustic pressure and velocity at inlet (subscript 2) and outlet (subscript 3) of a plain pipe of length L can be related by a transfer matrix, namely [8]

$$\begin{bmatrix} p_2 \\ \rho c u_2 \end{bmatrix} = \begin{bmatrix} \cos(kL) & \mathrm{i}\sin(kL) \\ \mathrm{i}\sin(kL) & \cos(kL) \end{bmatrix} \begin{bmatrix} p_3 \\ \rho c u_3 \end{bmatrix}, \tag{4}$$

where k is the wavenumber.

Let the holes have thickness t, the wall thickness of the perforated pipe. Typically t, b, $L < a$ and therefore, since this is a low-frequency plane-wave analysis, kt, kb, $kL \ll 1$. The specific impedance of a single aperture is then [9]

$$\zeta_h = \mathrm{i}k\left(t + \frac{16b}{3\pi\psi(\xi)}\right), \tag{5}$$

where [10] the Fok function $\psi(\xi)$, $\xi = b/B$, accounts for the interaction effects between holes and $B = \sqrt{(S/\pi)}$, where S is the zone area per hole. Explicitly,

$$\psi(\xi) = 1 + a_1\xi + a_2\xi^2 + a_3\xi^3 + a_4\xi^4 + \cdots;\ a_1 = -1.4092,\ a_2 = 0,\ a_3 = 0.338,\ a_4 = 0,$$
$$a_5 = 0.06793,\ a_6 = -0.2287,\ a_7 = 0.03015, \ldots .$$

It follows from Eqs. (3), (4) and (5), with only highest order terms retained, that

$$\begin{bmatrix} p_1 \\ \rho c u_1 \end{bmatrix} \approx \begin{bmatrix} 1 & \mathrm{i}kL \\ \dfrac{N}{\mathrm{i}k\left(t + 16b/3\pi\psi(\xi)\right)}\left(\dfrac{b}{a}\right)^2 & 1 + \dfrac{NL}{\left(t + 16b/3\pi\psi(\xi)\right)}\left(\dfrac{b}{a}\right)^2 \end{bmatrix} \begin{bmatrix} p_3 \\ \rho c u_3 \end{bmatrix}. \tag{6}$$

Let $\alpha = (Na/(t + (16b/3\pi\psi(\xi))))(b/a)^2$ and $\lambda = L/a$, both non-dimensional terms, then

$$\begin{bmatrix} p_1 \\ \mathrm{i}ka\rho c u_1 \end{bmatrix} \approx \begin{bmatrix} 1 & \lambda \\ \alpha & 1 + \alpha\lambda \end{bmatrix} \begin{bmatrix} p_3 \\ \mathrm{i}ka\rho c u_3 \end{bmatrix}. \tag{7}$$

This is the transfer matrix from inlet to outlet of a general jth section of the perforated tube. Since all n sections are identical and the outlet of one section is the inlet of the next, it follows that the transfer matrix from inlet plane I to outlet plane R of the perforated tube, see Fig. 4a, is given by

$$\begin{bmatrix} p_I \\ \mathrm{i}ka\rho c u_I \end{bmatrix} \approx \begin{bmatrix} 1 & \lambda \\ \alpha & 1 + \alpha\lambda \end{bmatrix}^n \begin{bmatrix} p_R \\ \mathrm{i}ka\rho c u_R \end{bmatrix}. \tag{8}$$

Let

$$\begin{bmatrix} A_n & B_n \\ C_n & D_n \end{bmatrix} = \begin{bmatrix} 1 & \lambda \\ \alpha & 1 + \alpha\lambda \end{bmatrix}^n, \tag{9}$$

then it follows from Eqs. (8) and (9) that the impedance at plane I

$$\zeta_I \equiv \frac{p_I}{\rho c u_I} \approx \mathrm{i}ka\left(\frac{A_n(\zeta_R/\mathrm{i}ka)+B_n}{C_n(\zeta_R/\mathrm{i}ka)+D_n}\right). \tag{10}$$

By definition, $\zeta_I = \mathrm{i}kl$, where l is the end correction, hence

$$l \approx a\left(\frac{A_n(\zeta_R/\mathrm{i}ka)+B_n}{C_n(\zeta_R/\mathrm{i}ka)+D_n}\right). \tag{11}$$

3. Experimental verification

The experiment consisted in measuring the resonant frequency of a Helmholtz resonator with a neck that consisted of a plain pipe section followed by a perforated pipe section, see Figs. 5 and 6. The perforated pipe terminated into free space, hence [1] $\zeta_R \approx \mathrm{i}0.61ka$ and it follows from Eq. (11) that

$$l \approx \left(\frac{0.61A_n + B_n}{0.61C_n + D_n}\right)a. \tag{12}$$

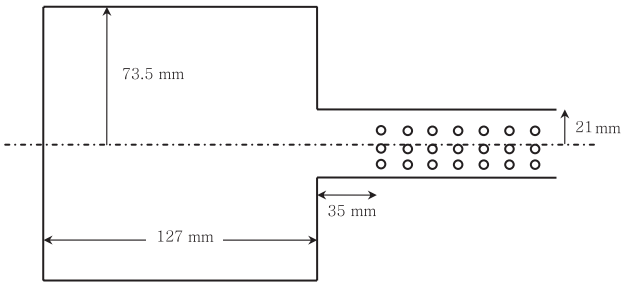

Fig. 5. Helmholtz resonator as used in the experiments.

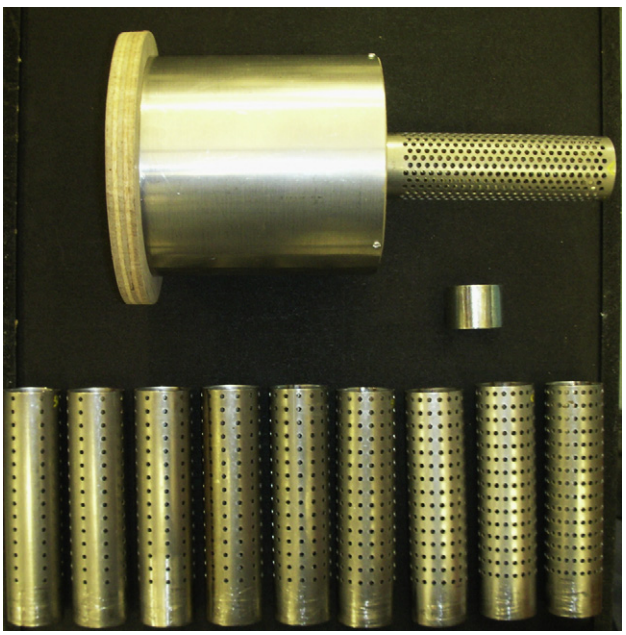

Fig. 6. Helmholtz resonator and the plain/perforated necks used in the experiments.

The resonator was placed inside an anechoic chamber within which white noise was generated in the free field by a loudspeaker. A microphone within the end wall of the resonator was used to measure the frequency response and the resonant frequency was taken as that of the peak response. Since the resonant frequency f of a Helmholtz resonator of volume V is given by

$$f = \frac{c}{2\pi}\sqrt{\frac{S}{l_{\text{eff}}V}}, \tag{13}$$

where $S = \pi a^2$ is the cross-sectional area of the neck and l_{eff} is its effective acoustic length, the measurement of f enabled the calculation of the total end correction l_{ec} given the actual length l_{act} of the plain neck section, since $l_{\text{ec}} = l_{\text{eff}} - l_{\text{act}}$. The end correction at the opening into the Helmholtz volume is simply that of a flanged pipe opening into half-space [2] modified by the Karal factor [3], namely $(8a/3\pi)H(\alpha)$. Since the ratio of duct radii α is 0.29 in this case, see Fig. 5, $H(\alpha) \approx 0.6$. The length of the Helmholtz chamber used here is sufficient for any change of this end correction due to the finite length of the chamber to be negligible [11]. Thus, the experimental value for the end correction l due to the perforated tube was evaluated as $l = l_{\text{eff}} - l_{\text{act}} - (8a/3\pi)H(\alpha)$.

Various different perforated sections were used as well as a simple plain tube without any perforate, see Fig. 6. In all cases, the length of the plain pipe section l_{act} was kept constant at 35 mm as measured to the centre of the first row of holes. The tube thickness was 1.5 mm and the radius of each hole 3.5 mm in every case, which are both very typical of automotive silencer applications.

In the first instance, the plain tube resonator neck shown in Fig. 6 was used as a check of the methodology. The known theoretical end correction [1] is $0.61a$. Four separate measured values gave a maximum difference in the measured resonant frequency of 1 Hz and corresponding values of the end correction between $0.59a$ and $0.62a$, with an average of $0.61a$. Thus, both accuracy and repeatability were found to be very good. The next test was for the perforate section shown attached to the resonator in Fig. 6, with 49 closely spaced staggered rings of holes, for which the axial ring-to-ring spacing $L = 2.85$ mm and the number of holes per ring $N = 13$. The resultant porosity of the perforate is 22%. The theoretical end correction for this perforate as given by Eqs. (9) and (11) is $0.90a$. Four different measurements were performed that resulted in resonant frequencies with a maximum difference of 1 Hz and corresponding values of the end correction between $0.93a$ and $0.97a$, with an average of $0.94a$. The theoretical value lies just outside the range of experimental values but, given the high porosity and the complexity of the hole pattern, the result is reasonable. It has been found in the course of this work that as the spacing between holes is reduced the precise theoretical value of end correction becomes dominated by the Fok function in Eq. (5), i.e. the interference effect between holes. The Fok function was

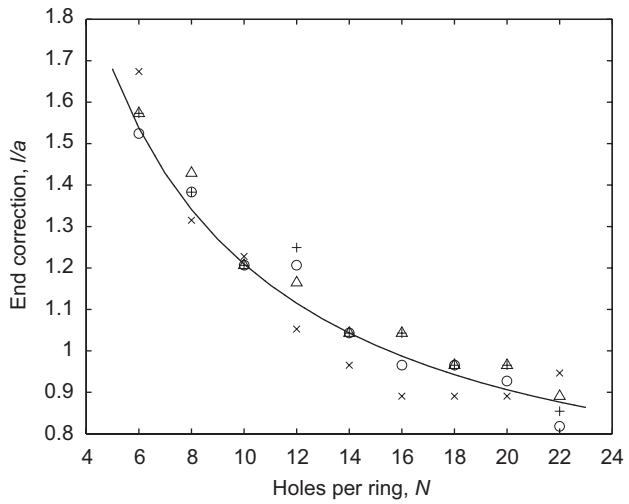

Fig. 7. Comparison of experimental (× , ◦, + , Δ) and theoretical ——, – – – – – values of end correction for a set of perforates with $n = 15$ that vary only in the number of holes per ring, N. —— Eqs. (9) and (12); – – – – – Eq. (18) (indistinguishable).

initially evaluated from consideration of a uniform pattern of holes and the later modification to specify a zone area per hole to enable use for non-uniform distributions is inexact. This is the most likely source of the small error seen in these results.

Finally, the set of nine similar perforates shown along the bottom of Fig. 6 were tested. For each of these perforates, the pattern of holes is rectangular, the ring spacing $L = 10\,\text{mm}$ and the number of rings $n = 15$. They differ only in the number of holes per ring N, which varies from 6 to 22 with a corresponding variation of porosity from 4.4% to 16.1%, a range which encompasses values normally used in automotive silencer applications. Four sets of test results were found for this group of perforates and the resultant values for end correction are shown in Fig. 7, together with the theoretical values from Eqs. (9) and (12). The theoretical results are seen to lie within the error bounds of the experimental results and to display exactly the right characteristics.

4. Further analytical results

In practical situations, it is not usual for a perforated pipe to terminate in an open end that radiates into free space, such as in the case of the experiments in Section 3. The normal situation is for a perforated section of pipe to bridge two plain sections of pipe, as in the examples of Figs. 2 and 3. In such a situation, the theoretical end correction is given by Eq. (11) but in practice the termination impedance ζ_R can only be found by complete analysis of much of the silencer system, which then detracts from the advantage of using end corrections. Thus, the theory only becomes usefully applicable in the general situation once the length of a given perforate is sufficient for the reactance at the 'far' end of the perforate, plane R, to be inconsequential. This effect is demonstrated in Fig. 8, which shows the end correction as a function of the number of rings of holes n in the perforate. The hole size, linear spacing and general pattern are the same as those for the test results of Fig. 7. Three sets of results are shown for differing numbers of holes per ring, N. As one might expect, the end correction becomes constant after a fewer number of rings of holes as the number of holes per ring increases. For the worst case considered, $N = 5$, the end correction is essentially constant once the number of rings $n = 8$ or more. A value of $N = 5$ corresponds to a porosity of less than 4%, which is below that used in normal applications, while perforates would ordinarily consist of far more than 8 rings of holes.

It might be argued that the convergence of the end correction to a constant value as n increases is not in itself sufficient proof that the value of the termination impedance ζ_R is therefore inconsequential, but simply has constant effect. Thus, as a further check the calculations that underpin Fig. 8 were repeated for several different values of ζ_R. It was found that the results converged to the same value and at virtually the same rate whatever the value of ζ_R.

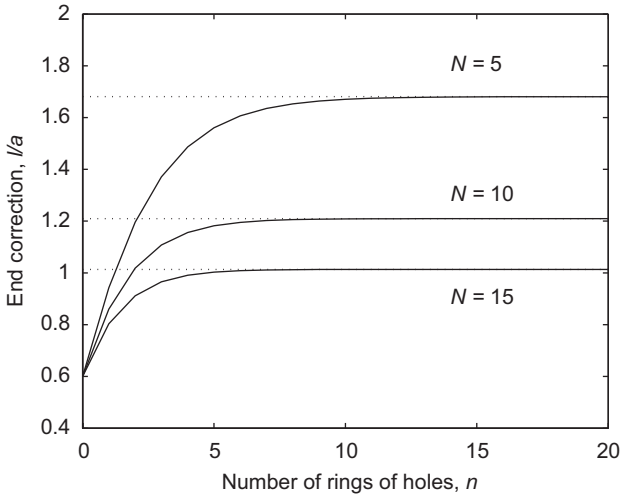

Fig. 8. End correction as a function of the number of rings of holes, n, for various numbers of holes per ring, N. —— Eqs. (9) and (12); – – – – – large n limit of Eq. (18).

For the perforates used in the experiments $n = 15$ or more and hence it follows from above that the fact that the perforate terminated into free space should be irrelevant. In a few cases, the experiment was repeated with the open end blanked off by a solid plate or filled with foam to reaffirm this conclusion and there was no noticeable change of resonant frequency.

The observations above together with Eq. (11) indicate that the converged value of the end correction for large n must be given either by

$$l \approx \frac{A_n}{C_n} a \quad \text{or} \quad l \approx \frac{B_n}{D_n} a. \tag{14a, b}$$

It transpires that both of these equations are valid and give the correct converged value of end correction, with Eq. (14b) converging slightly the quicker of the two and having less error for small n.

While the end correction given by Eqs. (11) or (14) can be rapidly evaluated on a computer, it is not readily found by a calculator nor is it possible to see directly the influence of all of the various parameters in the problem. Thus, it is of value to investigate approximations they may fulfil these goals and remain of acceptable accuracy. Towards this end, it can readily be shown following Eq. (9) that

$$\begin{bmatrix} 1 & \lambda \\ \alpha & 1+\alpha\lambda \end{bmatrix}^n = \beta_n \begin{bmatrix} 1 & \lambda \\ \alpha & 1+\alpha\lambda \end{bmatrix} - \beta_{n-1} \begin{bmatrix} 1 & 0 \\ 0 & 1 \end{bmatrix}, \tag{15}$$

where $\beta_n = (2+\alpha\lambda)\beta_{n-1} - \beta_{n-2}$, $\beta_1 = 1$, $\beta_0 = 0$. Thus,

$$\frac{l}{a} \approx \frac{(\zeta_R/\mathrm{i}ka)(1-\beta_{n-1}/\beta_n)+\lambda}{\alpha((\zeta_R/\mathrm{i}ka)+\lambda)+(1-\beta_{n-1}/\beta_n)}. \tag{16}$$

Eq. (16) gives exactly the same values as Eqs. (9) and (11) but is still not readily calculated for large n. However, it follows from the remarks prior and subsequent to Eq. (14) that in the converged limit for large n

$$\frac{l}{a} \approx \frac{(1-\beta_{n-1}/\beta_n)}{\alpha} \approx \frac{\lambda}{\alpha\lambda+(1-\beta_{n-1}/\beta_n)}. \tag{17}$$

The two expressions of Eq. (17) enable one to remove the problematic term involving the ratio of β_{n-1}/β_n and this results in a very simple formula for the converged value of end correction, namely

$$\frac{l}{a} \cong \frac{\lambda}{2}\left(\sqrt{1+\frac{4}{\alpha\lambda}}-1\right) = \frac{L}{2a}\left(\sqrt{1+\frac{4\{t+16b/[3\pi\psi(\xi)]\}}{NL}\left(\frac{a}{b}\right)^2}-1\right). \tag{18a, b}$$

Thus, not only is the end correction readily computed by Eq. (18a) but it is also a simple enough formula for the dependence of the various parameters to be explicitly seen, as in Eq. (18b). When Eq. (18a, b) is used to compute the end correction to compare with the experimental results in Fig. 7, for which $n = 15$, the values are indistinguishable from those obtained via the complete analysis of Eqs. (9) and (11). The convergence towards this limit approximation for large n is shown in Fig. 8 for different values of N.

In some theoretical analyses of perforates, the impedance of the holes has to be uniformly distributed or smeared over the surface of the perforate. In the plane-wave decoupling approach [5] a uniform axial and circumferential distribution is assumed while in the finite element results for end corrections [6] a uniform circumferential distribution is used because of the assumed axisymmetry for the problem. Even in the segmentation approach [4], it has not been deemed necessary to match the number of segments with the number of rings of holes. The effect is to make the linear spacing L between rings of holes and/or the number of holes per ring N irrelevant, such that the actual pattern of holes is disregarded and the single relevant parameter becomes the porosity of the perforate. In the more general theory given in Section 2, both L and N are retained and it is therefore possible, for a given size of holes, to consider perforates of the same porosity with differing patterns of holes. Fig. 9 shows results of end correction versus N for different porosities of perforate, i.e. L is automatically adjusted with N. In all these results $n = 15$ such that the open end condition has no influence. It is seen that the maximum variation of end correction for a given constant porosity increases as the porosity reduces but that even for normal levels of porosity between 10% and 15%, there is a

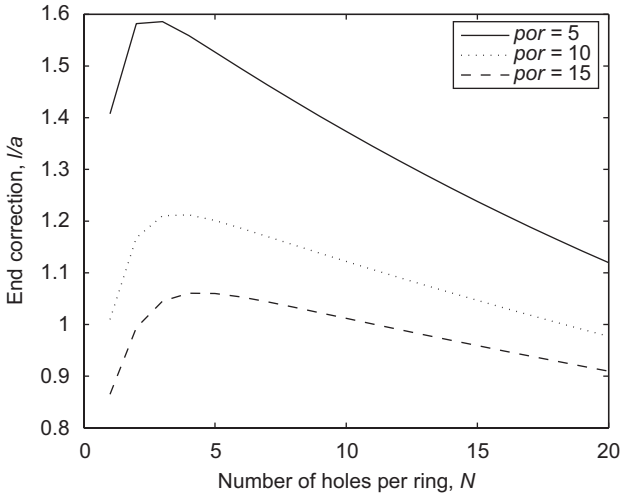

Fig. 9. End correction as a function of the number of holes per ring, N, for various values of percentage porosity (por).

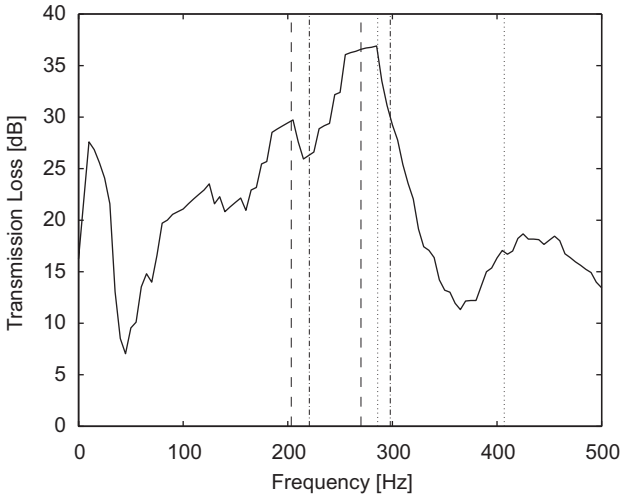

Fig. 10. Measured transmission loss of a triple-pass silencer, showing predicted resonant frequencies of the reversal chambers: --------- no end corrections; –·–·–·– plain tube end corrections; – – – – – perforate and plain tube end corrections.

noticeable effect on the end correction. The conclusion is that to get very accurate analysis of the effects of perforates it is necessary to account for the precise distribution of holes in the analysis.

Finally, a practical example of the significance of using precise end corrections can be seen in Fig. 10, which shows the measured transmission loss of a triple-pass silencer of the generic type as shown in Fig. 3. The silencer is a 14.5 l rear-box unit for a passenger vehicle, the data for perforates being $N = 12$, $b = 1.75$ mm, $t = 1.5$ mm and $L = 11.7$ mm, giving 6% porosity. The reversing chambers have internal volumes of 4.11 and 3.16 l. Three of the four necks to these chambers have plain pipe neck lengths of 23 mm, the fourth has length 80 mm and is one of the two necks for the larger chamber. All perforated and plain pipes have internal diameter of 51 mm. Without use of end corrections, the large and small chambers are predicted to have resonant frequencies of 286 and 407 Hz, respectively. If plain tube end corrections are used at both ends of each neck, suitably modified by the Karal factor of 0.65 in this instance, the predicted frequencies are 220.6 and 298 Hz, respectively. Finally, if Eq. (18b) is used to evaluate the end correction at the perforate and the plain tube end correction is used at the other end of each neck, both modified by the Karal factor, the predicted frequencies are 203.4 and 270 Hz, respectively. It can be seen from Fig. 10 that the latter values

coincide extremely closely with the maxima in the measured transmission loss results due to resonance in the two reversing chambers. In contrast, use of plain tube end corrections gives appreciable error and neglect of end corrections leads to meaningless results.

5. Conclusions

A general formula for the plane-wave end correction that should be applied at the junction of a plain and a perforated pipe of equal diameter has been derived and verified by experimental results with reference to a Helmholtz resonator. The formula only becomes of full practical benefit once the perforate is long enough for the termination condition at the opposite end to the junction with the plain pipe to become irrelevant. It has been shown that for the type and size of perforated pipes that are normal in automotive silencer applications this condition is generally met. A simple expression that evaluates this long length limit has been evaluated and is of closed form such that the dependence of the end correction upon the various parameters within the problem becomes explicit. It is also shown that if accurate results are required for the acoustic analysis of perforates the distribution of holes must be correctly modelled and the porosity alone is insufficient. Perforated pipes are normally used in silencers because of the presence of mean flow. The influence of mean flow upon the end correction remains to be investigated.

Acknowledgments

The author wishes to thank Mr. A. Blackford of Loughborough University who was responsible for many of the experimental measurements.

References

[1] M. Levine, J. Schwinger, On the radiation of sound from an unflanged circular pipe, *Physical Review* 73 (1948) 383–406.
[2] J.W.S. Rayleigh, *Theory of Sound*, second ed., Macmillan, New York, 1894 Art 307–314.
[3] F.C. Karal, The analagous acoustical impedance for discontinuities and constrictions of circular cross section, *Journal of the Acoustical Society of America* 25 (1953) 327–334.
[4] J.W. Sullivan, A method of modelling perforated tube muffler components. I. Theory, *Journal of the Acoustical Society of America* 66 (1979) 772–778.
[5] K.S. Peat, A numerical decoupling analysis of perforated pipe silencer elements, *Journal of Sound and Vibration* 123 (1988) 199–212.
[6] A.J. Torregrosa, A. Broatch, R. Payri, F. Gonzalez, Numerical estimation of end corrections in extended-duct and perforated-duct mufflers, *Transactions of the ASME* 121 (1999) 302–308.
[7] K.S. Peat, End corrections due to perforated pipes, *Bulletin of the Institute of Acoustics* 33 (1) (2008) 22–25.
[8] M.L. Munjal, *Acoustics of Ducts and Mufflers*, Wiley, New York, 1987.
[9] T.H. Melling, The acoustic impedance of perforates at medium and high sound pressure levels, *Journal of Sound and Vibration* 29 (1973) 1–65.
[10] S.N. Rschevkin, *A Course of Lectures on the Theory of Sound*, Pergamon Press, London, 1963.
[11] Zhongxu Kang, Zhenlin Ji, Acoustic length correction of duct extension into a cylindrical chamber, *Journal of Sound and Vibration* 310 (2008) 782–791.